Cell Reports
Medicine

Article

Mucosal chemokine adjuvant enhances synDNA vaccine-mediated responses to SARS-CoV-2 and provides heterologous protection *in vivo*

Graphical abstract

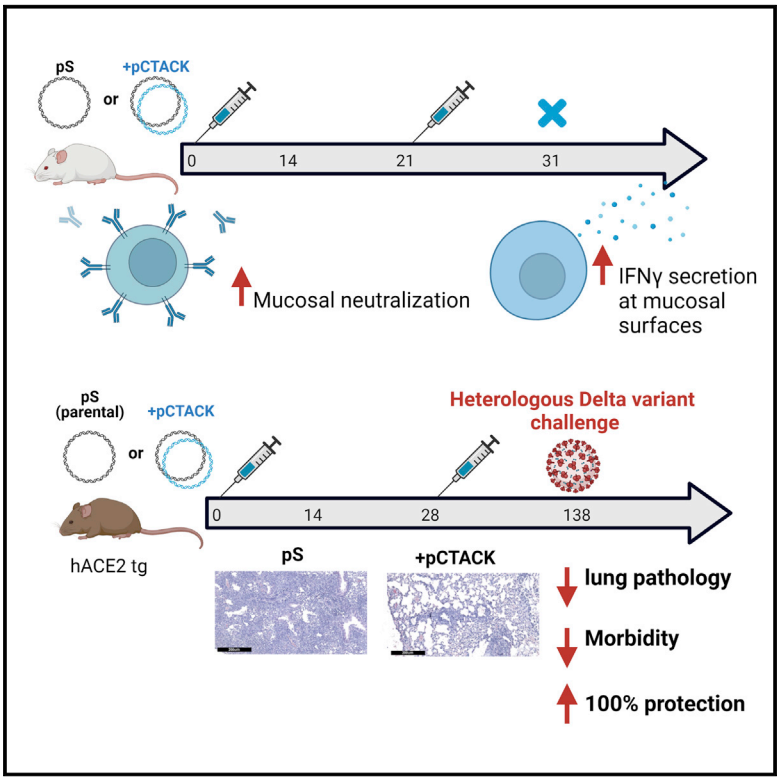

Highlights

- Mucosal chemokine CCL27 (CTACK) enhances SARS-CoV-2 DNA vaccine-induced responses
- CTACK co-delivery confers 100% protection from SARS-CoV-2 VOC challenge
- Enhanced mucosal immunity may support broad protection from SARS-CoV-2 variants

Authors

Ebony N. Gary, Nicholas J. Tursi, Bryce Warner, ..., Ami Patel, Daniel W. Kulp, David B. Weiner

Correspondence

dweiner@wistar.org

In brief

Gary et al. describe how co-immunization with a spike protein DNA vaccine and the mucosal-homing chemokine CCL27 enhances SARS-CoV-2 vaccine-induced responses in the respiratory and gastrointestinal mucosae and supports protection from the SARS-CoV-2 Delta variant. These studies suggest that mucosal targeting may play an important role in broadening vaccine-induced protection against SARS-CoV-2.

Gary et al., 2022, Cell Reports Medicine *3*, 100693
July 19, 2022
https://doi.org/10.1016/j.xcrm.2022.100693

CellPress

Cell Reports Medicine

CellPress
OPEN ACCESS

Article

Mucosal chemokine adjuvant enhances synDNA vaccine-mediated responses to SARS-CoV-2 and provides heterologous protection *in vivo*

Ebony N. Gary,[1,7] Nicholas J. Tursi,[1,2,7] Bryce Warner,[3] Elizabeth M. Parzych,[1] Ali R. Ali,[1] Drew Frase,[1] Estella Moffat,[4] Carissa Embury-Hyatt,[4] Trevor R.F. Smith,[5] Kate E. Broderick,[5] Laurent Humeau,[5] Darwyn Kobasa,[3,6] Ami Patel,[1] Daniel W. Kulp,[1] and David B. Weiner[1,8,*]

[1]The Vaccine and Immunotherapy Center, The Wistar Institute, Philadelphia, PA, USA
[2]Perelman School of Medicine, University of Pennsylvania, Philadelphia, PA, USA
[3]Special Pathogens Program, National Microbiology Laboratory, Public Health Agency of Canada, Winnipeg, MB, Canada
[4]National Center for Foreign Animal Disease (NCFAD), Canadian Food Inspection Agency, Winnipeg, MB, Canada
[5]Inovio Pharmaceuticals, Bluebell, PA, USA
[6]Department of Medical Microbiology and Infectious Diseases, University of Manitoba, Winnipeg, MB, Canada
[7]These authors contributed equally
[8]Lead contact
*Correspondence: dweiner@wistar.org
https://doi.org/10.1016/j.xcrm.2022.100693

SUMMARY

The global coronavirus disease 2019 (COVID-19) pandemic has claimed more than 5 million lives. Emerging variants of concern (VOCs) continually challenge viral control. Directing vaccine-induced humoral and cell-mediated responses to mucosal surfaces may enhance vaccine efficacy. Here we investigate the immunogenicity and protective efficacy of optimized synthetic DNA plasmids encoding wild-type severe acute respiratory syndrome coronavirus 2 (SARS-CoV-2) spike protein (pS) co-formulated with the plasmid-encoded mucosal chemokine cutaneous T cell-attracting chemokine (pCTACK; CCL27). pCTACK-co-immunized animals exhibit increased spike-specific antibodies at the mucosal surface and increased frequencies of interferon gamma (IFNγ)$^+$ CD8$^+$ T cells in the respiratory mucosa. pCTACK co-immunization confers 100% protection from heterologous Delta VOC challenge. This study shows that mucosal chemokine adjuvants can direct vaccine-induced responses to specific immunological sites and have significant effects on heterologous challenge. Further study of this unique chemokine-adjuvanted vaccine approach in the context of SARS-CoV-2 vaccines is likely important.

INTRODUCTION

Severe acute respiratory syndrome coronavirus 2 (SARS-CoV-2) emerged in the human population in December 2019 and spread rapidly, causing a global pandemic. To date, coronavirus disease 2019 (COVID-19) has infected more than 200 million people and killed more than 5 million people. Despite the rapid advancement of therapeutic agents and vaccine candidates to the clinic, the continued emergence of SARS-CoV-2 variants of concern (VOCs), the observed decline in vaccine[1–3] and infection-induced[4] antibody responses, and the sub-optimal responses of elderly individuals[5,6] to vaccine antigens continues to challenge viral control. Although studies have demonstrated the ability of currently authorized vaccines to prevent infection and severe illness among vaccinees,[7,8] studies to determine vaccine effectiveness against transmission (VET) have demonstrated modest efficacy at preventing transmission from index cases to vaccinated and unvaccinated household members during the Alpha and Beta variant infection waves.[9] Follow-up studies performed during the Delta variant infection wave detected markedly lower VET.[10] Vaccine strategies for improving SARS-CoV-2 infection control and potentially decreasing replication of SARS-CoV-2 at important sites associated with acquisition of infection and transmission will likely benefit from generation of improved immune responses at mucosal surfaces.

Systemic immunization induces robust humoral and cell-mediated immunity, which typically results in transudation of antibody to mucosal surfaces and transient entry of peripherally primed, short-lived effector T cells to mucosal surfaces. Peripheral immunization rarely induces *de novo* mucosal immune responses or mucosa-specific, tissue-resident memory T cells.[11,12] Thus, generating vaccine-induced responses specifically within mucosal compartments has remained a challenge for vaccines targeting mucosal pathogens. Peripherally primed effector cells are excluded from the mucosal compartment because of their lack of expression of mucosa-homing chemokine receptors. Vaccination approaches such as the "prime and pull" method, which specifically directs peripherally activated cells to the mucosa by applying mucosal chemokines after parenteral immunization,[13,14] enable chemokine ligands to be

studied as a tool to successfully direct vaccine responses to mucosal surfaces.

CC-chemokine receptor-10 (CCR10) is implicated in regulating mucosal and epithelial immunity through localization and maintenance of B cells and various T cell subsets.[15,16] CCR10 is the receptor for CCL27 (cutaneous T cell-attracting chemokine [CTACK]) and CCL28 (mucosal-associated epithelial chemokine [MEC]). CTACK is a 112-amino-acid chemokine expressed by epithelial cells, including keratinocytes, and is associated with recruitment and homing of T cells to the skin.[17,18] In tuberculosis-infected macaques, CTACK has been shown to be upregulated in the bronchial lymph nodes and lungs, suggesting a mucosal role of CTACK and its cognate receptor CCR10[19] in lung trafficking. CCR10 expression is closely associated with immunoglobulin A (IgA)-secreting B cells present at mucosal surfaces.[15,20,21] We previously reported that co-immunization with CCR10 ligands can modulate antigen-specific responses at mucosal surfaces, including the intestinal, vaginal, and lung mucosae.[22–24]

Considering the important role of mucosal surfaces in SARS-CoV-2 infection, we hypothesized that co-immunization of plasmid-encoded SARS-CoV-2 spike protein (pS) with plasmid-encoded CTACK (pCTACK) by highly efficient DNA delivery via 3P electroporation (EP) could enhance anti-SARS-CoV-2 humoral and cellular responses, including at the mucosa. Mice were immunized with pS alone or co-immunized with pS and pCTACK to determine antigen-specific cellular and humoral responses in the mucosa and periphery. pCTACK co-immunization enhanced cellular responses in the periphery and mucosa of co-immunized animals and enhanced humoral responses specifically in the mucosal compartment, including production of anti-SARS-CoV-2 neutralizing antibodies. pS DNA vaccination alone was highly effective in protecting more than 60% of animals from heterologous challenge with Delta variant SARS-CoV-2. Strikingly, 100% of animals co-immunized with pCTACK were protected from morbidity and mortality. These data indicate that pCTACK and perhaps other mucosal chemokines can be used to direct antigen-specific responses to distinct anatomical sites via peripheral immunization and potentially improve vaccine outcomes against SARS-CoV-2 variants.

RESULTS

pCTACK co-immunization enhances T cell responses in the mucosa and periphery

To determine whether CTACK co-immunization would affect mucosal T cell responses, mice were immunized twice, separated by 3 weeks, with 40 μg of empty plasmid vector (pVax), 10 μg of a synDNA plasmid encoding the full-length pS containing a D>G mutation at position 614 (pS) and 30 μg of pVax or co-immunized with 10 μg of pS and 30 μg of plasmid-encoded mouse CTACK (+pCTACK) (Figure 1A). On day 10 after the second immunization, animals were euthanized, and T cell responses were measured by interferon gamma (IFNγ) enzyme-linked immunosorbent spot (ELISpot) assay. Consistent with previous reports,[25] we observed that pS-immunized animals displayed robust spike-specific IFNγ responses in the spleen (Figures 1B–1D) and lungs (Figures 1C–1E) compared with animals immunized with pVax. However, co-immunization of pS with pCTACK resulted in statistically significant increases in IFNγ secretion in the spleen (Figures 1B–1D) and lungs (Figures 1C–1E) compared with animals receiving pS alone. This enhancement was observed across multiple spike antigen pools, supporting the diversity of engaged T cells. We quantified antigen-specific $CD8^+$ T cell responses using intracellular flow cytometry in the spleen and lungs of immunized mice. We observed a trend toward increased frequencies of T cells expressing $\alpha4\beta7$ integrin, a hallmark of mucosal priming and a requirement for mucosal maintenance (Figure 1F).[26,27] Among lung $\alpha4\beta7^+$ $CD8^+$ T cells in the lungs, we observed a significant increase in IFNγ secretion from T cells of pCTACK co-immunized animals in response to spike peptide pools compared with pS-only-immunized animals (Figure 1G). We detected no differences in IFNγ secretion from $\alpha4\beta7^+$ $CD8^+$ T cells in the lungs of pS-immunized and control-immunized animals (Figure 1G). In the spleen, pCTACK co-immunization resulted in a significant decrease in the frequency of $\alpha4\beta7^+$ T cells (Figure 1H). These data suggests that pCTACK co-immunization supports the direction of lymphocytes from the periphery toward the mucosa. Among lung $\alpha4\beta7^+$ $CD8^+$ T cells in the spleen, we observed no differences in IFNγ secretion from T cells of pCTACK-co-immunized animals compared with pS-only-immunized animals (Figure 1I). These results support the theory that molecular plasmid co-immunization with this CCR10 ligand in the periphery enhances antigen-specific T cell responses in peripheral and SARS-CoV-2-relevant mucosal compartments.

pCTACK immunization increases SARS-CoV-2-specific mucosal antibody responses

We hypothesized that pCTACK co-immunization would enhance SARS-CoV-2 specific antibodies at mucosal surfaces and enhance anti-SARS-CoV-2 IgA antibody formation in these sites. Mice were immunized as shown in Figure 1A, and antigen-specific antibodies were measured in serum after two immunizations (Figures 2A–2D). Immunization with spike DNA alone resulted in significant increases in spike receptor binding domain (RBD)-specific IgG2a (Figure 2B), IgG2b (Figure 2C), and total IgG (Figure 2D) in the serum of immunized mice. Compared with naive animals, pCTACK co-immunization significantly increased antigen-specific IgG1 (Figure 2A), IgG2a (Figure 2B), and total IgG (Figure 2D). We observed no differences in total IgG or IgG isotypes between pS-only and pCTACK co-immunized animals. Similarly, serum levels of spike-specific IgA were comparable between pS-only- and pCTACK-co-immunized mice (Figure 2E). We determined the ability of serum from immunized animals to neutralize SARS-CoV-2 pseudotyped viruses *in vitro*. Serum from animals immunized with pS alone and co-immunized with pS and pCTACK were equally capable of neutralizing SARS-CoV-2 pseudotyped viruses (Figure 2F). Similarly, serum from pS-immunized and pCTACK co-immunized mice were equally capable of neutralizing live parental (Figure 2G) and Delta VOC viruses (Figure 2H). These data indicate that pCTACK co-immunization does not significantly augment serological responses.

Because CCR10 expression is closely associated with IgA^+ B cells at mucosal surfaces, we hypothesized that pCTACK co-administration might affect anti-SARS-CoV-2 mucosal immunity. We

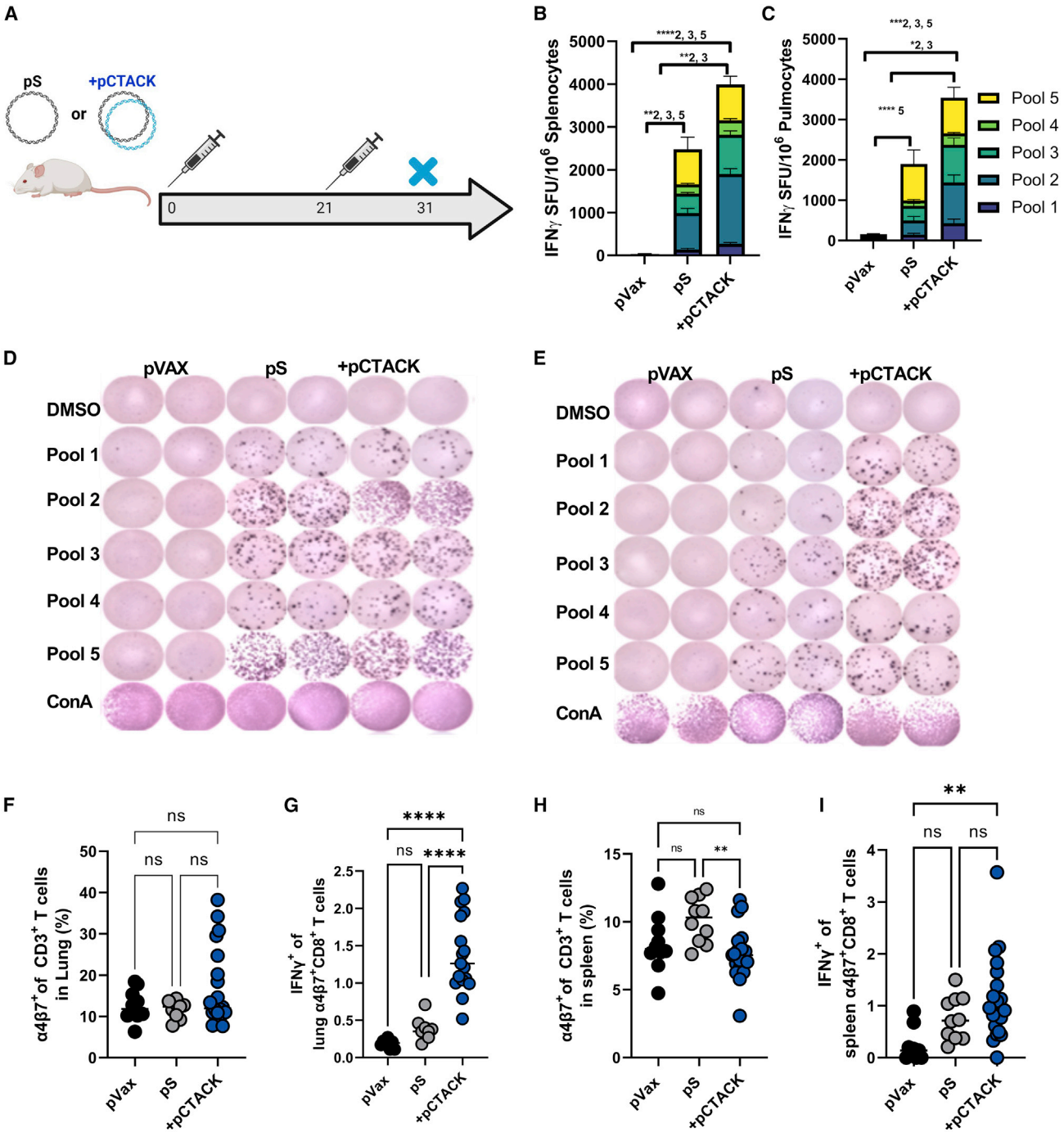

Figure 1. pCTACK enhances IFNγ secretion *in vivo*

(A) Mice were immunized twice, separated by 3 weeks, with 40 μg of empty plasmid (pVax) or 10 μg of SARS-CoV-2 spike DNA vaccine alone or co-immunized with pS and 30 μg cutaneous T cell-attracting chemokine DNA (+pCTACK).

(B–E) Lymphocytes in the spleens (B–D) and lungs (C–E) were stimulated with overlapping peptide pools representing the full-length spike glycoprotein and subjected to an IFNγ ELISpot assay on day 11 after the second immunization.

(F–I) Lung (F and G) and spleen (H and I) lymphocytes were subjected to SARS-CoV-2 peptide stimulation for 6 h, and intracellular cytokine staining was used to detect the frequencies of $\alpha4\beta7^+$ T cells (F–H) and $\alpha4\beta7^+$ IFNγ-secreting $CD8^+$ T cells (G and I) in these compartments.

Bars represent the mean, and error bars represent SD (B and C). Symbols represent individual animals, and bars represent SD (F–I). Data are representative of 2 (B–E) or 1 (F–I) independent experiment(s) (n = 5–20 mice/group). *p < 0.05, **p < 0.01, ***p < 0.001, ****p < 0.0001 by two-way ANOVA (B and C) or Kruskal-Wallis ANOVA (F–I).

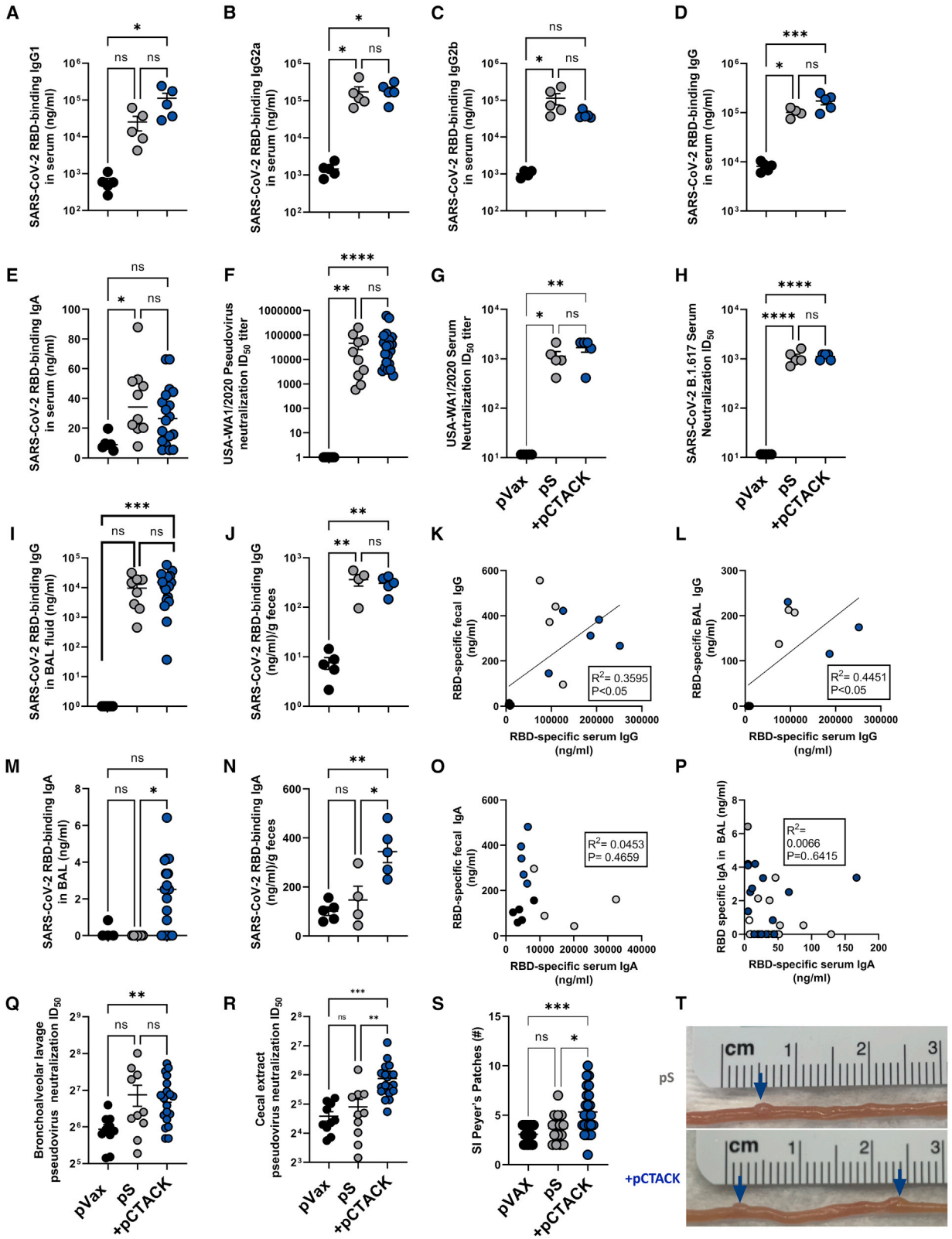

(legend on next page)

observed no differences in SARS-CoV-2-specific IgG in bronchoalveolar lavage (BAL) or fecal extracts between pS-only- and pCTACK-co-immunized animals (Figures 2I and 2J). IgG induced by peripheral vaccination can passively transudate to mucosal surfaces, resulting in increased antigen-specific IgG in the mucosa. In support of this, serum IgG levels strongly correlated with cecal (Figure 2K) and BAL (Figure 2L) IgG levels. Co-immunization with pCTACK induced significantly more RBD-specific IgA in BAL (Figure 2M) and cecal extracts (Figure 2N) than immunization with pS alone. In the case of antigen-specific IgA, there was no correlation between serum IgA levels and levels of IgA in the cecal extract (Figure 2O) or BAL (Figure 2P) of immunized animals. We determined the capacity of BAL (Figure 2Q) and cecal extract (Figure 2R) from immunized animals to neutralize pseudotyped virus. Co-immunization with pCTACK led to an increase in neutralization capacity over control-immunized animals at both sites (Figures 2Q and 2R) but was only significantly increased, compared with pS-only immunized animals, in the intestinal compartment (Figure 2R). In support of increased intestinal mucosal responses, we also observed an increase in the number of small intestinal Peyer's patches in pCTACK co-immunized animals (Figures 2S and 2T). These data support the theory that pCTACK enhances mucosal responses, including IgA responses, via a distinct immunological phenomenon and not passive diffusion of increased peripheral IgA.

pCTACK co-immunization is protective in heterologous SARS-CoV-2 challenge

To determine the effect of pCTACK co-immunization on infection outcome, human ACE2 transgenic (hACE2tg) mice were immunized with pS alone or co-immunized with +pCTACK on days 0 and 28. 110 days after the final immunization, animals were heterologously challenged with 1×10^5 $TCID_{50}$ of SARS-CoV-2 (Delta) (Figure 3A). Antibody function was measured via pseudovirus neutralization assay prior to challenge on day 90 after the second immunization. As shown in Figure 2, pCTACK-co-immunized animals and pS-only-immunized animals exhibited similar levels of wild-type (Figure 3B) and Delta VOC (Figure 3C) pseudovirus neutralization capacity prior to challenge. Representative animals from each group were euthanized at the peak of infection, 4 days after challenge, and viral loads were measured via TCID50 assay and qPCR for viral RNA. The remaining six animals from each group were monitored daily for weight loss until the study endpoint. All immunized animals exhibited lower viral loads, as measured by TCID50 (Figure 3D) and qPCR (Figure 3E), compared with control animals. Although there was a clear trend toward decreased viral RNA in the lungs of pCTACK co-immunized animals, there was no significant difference in viral loads, as measured by TCID50 (Figure 3D) or qPCR (Figure 3E), between animals immunized with pS alone or those co-immunized with pCTACK. Significant weight loss and mortality was observed among pVax-immunized animals (Figures 3F–3I). Among pS-only immunized mice, significant weight loss was observed, and two animals succumbed to infection, but the majority of animals recovered from infection-induced weight loss (Figures 3G–3I). No weight loss was observed among pCTACK co-immunized animals after Delta variant challenge (Figures 3H and 3I). We observed 100% mortality among control-plasmid-immunized mice, 40% mortality among pS-immunized mice, and 0% mortality among animals co-immunized with +pCTACK (Figure 3J). We evaluated lung pathology 4 days after challenge in four euthanized mice from each group and scored the sections for percentage of area affected, the presence of interstitial pneumonia, and evidence of vascular lesions. pCTACK-co-immunized mice had significantly lower pathology scores (Figure 3K). In the sections from these mice, we observed significant lung involvement among pVax- and pS-only-immunized mice as well as the presence of vasculitis and type II pneumocyte infiltration, whereas pCTACK co-immunized mice had decreased lung lobe involvement and minimal inflammatory infiltrates (Figure 3L). When lung sections were stained for SARS-CoV-2 nucleocapsid (N) antigen, we observed robust positive staining in all pVax-immunized mice and minimal staining in all pS-only-immunized mice and were only able to detect minimal staining in 2 of the 4 evaluated mice in the pCTACK-co-immunized group (Figure 3L). These data suggest that pCTACK co-immunization has a significant effect on heterologous challenge outcomes.

DISCUSSION

Chemokines, cytokines, and their receptors play important roles in lymphocyte development, migration, function, and homeostasis; thus, they have significant therapeutic potential.[28] Promising preclinical data from our lab and others suggests that co-delivery of chemokines and cytokines as vaccine adjuvants can significantly affect immune responses[23,29–32] and challenge outcomes.[22] The reported prime-and-pull method of applying chemokines to mucosal surfaces after parenteral immunization to recruit activated lymphocytes to relevant mucosal surfaces has

Figure 2. pCTACK enhances anti-SARS-CoV-2 mucosal humoral responses

(A–E) Mice were immunized as shown in Figure 1A, and SARS-CoV-2 receptor binding domain (RBD)-specific IgG1 (A), IgG2a (B), IgG2b (C), total IgG (D), and IgA (E) were quantified by ELISA.

(F) SARS-CoV-2 serum pseudovirus neutralization ID50 titer.

(G and H) SARS-CoV-2 Washington (G) and Delta variant (H) live virus neutralization.

(I and J) SARS-CoV-2 RBD binding IgG in bronchoalveolar lavage (BAL) (I) and cecal extracts (J).

(K and L) Spearman correlations between serum IgG and cecal extract IgG (K) and BAL fluid (L).

(M and N) SARS-CoV-2 RBD binding IgA in BAL (M) and cecal extract (N).

(O and P) Spearman correlation between serum IgA and cecal extract (O) and BAL IgA (P).

(Q and R) BAL (Q) and cecal extract (R) pseudoviral neutralization ID50 values.

(S and T) Quantification of small intestinal (SI) Peyer's patches (S) and representative Peyer's patches (blue arrows) (T).

Each symbol is the average of duplicate assays for one mouse (A–R) or a single mouse (S and T). Horizontal lines represent the mean, and error bars represent SEM (A–R) or SD (S). Data are representative of 2 independent experiments (n = 5–20 mice/group). *$p < 0.05$, **$p < 0.01$ by Kruskal-Wallis ANOVA.

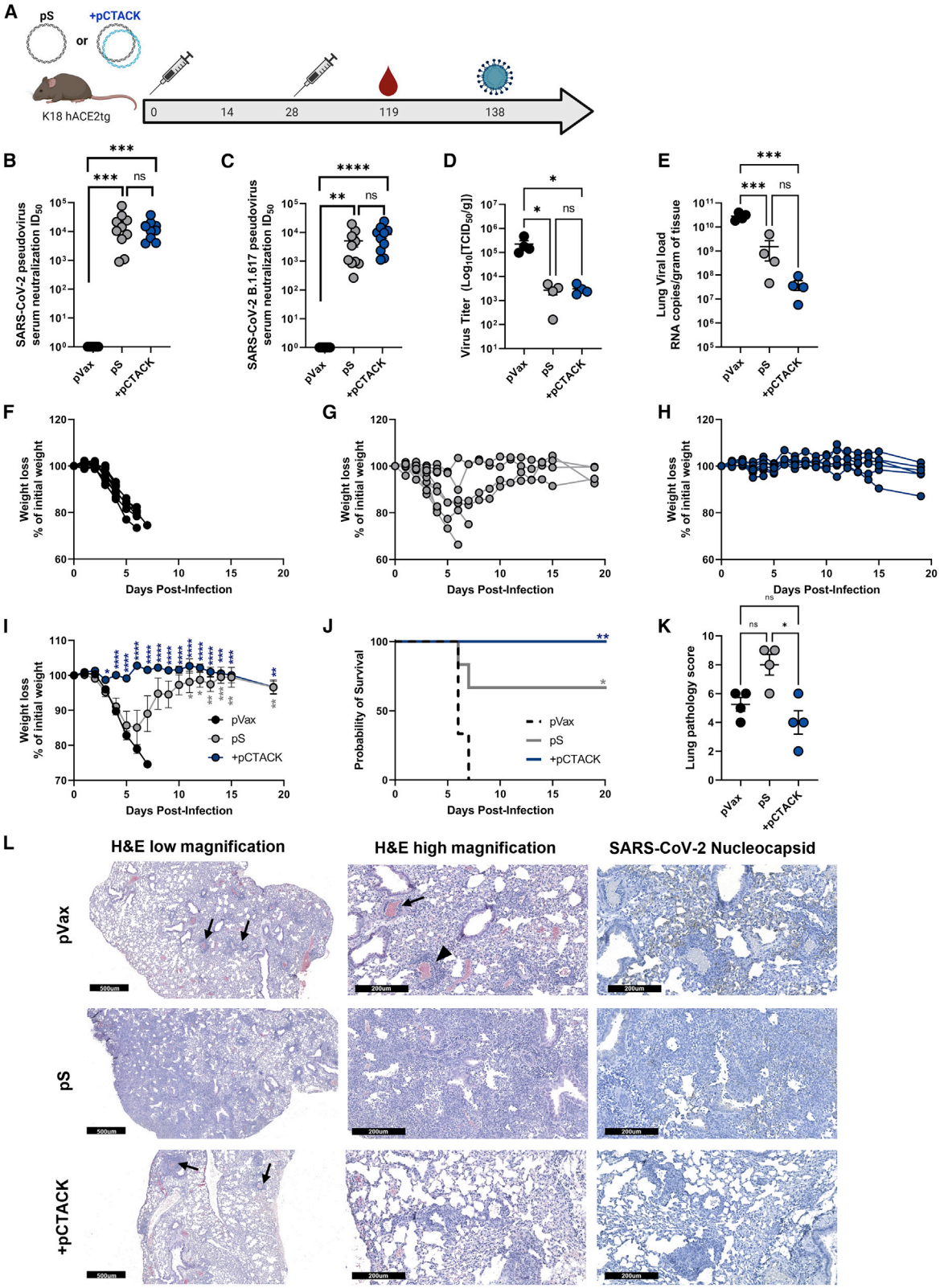

(legend on next page)

demonstrated significant preclinical efficacy.[14,33] However, few clinical studies evaluating the effect of chemokine or cytokine co-administration in a vaccine setting have been performed. In the infectious disease space, we have determined that co-delivery of plasmids encoding human interleukin-12 (IL-12) enhances cellular and humoral responses to synDNA antigens in affected individuals.[34] Similarly, we recently reported on the ability of co-delivered human IL-12 to enhance cellular responses targeting solid tumors in individuals with cancer.[35] A clinical trial (ClinicalTrials.gov: NCT01433172), focused on delivery of cells expressing CD40L and CCL21 to recruit and activate T cells in the context of lung cancer, has recently been completed. The authors reported a significant increase in tumor-infiltrating T cells in the presence of CCL21.[36] These clinical results suggest that the immunomodulatory effects of chemokines and cytokines can be harnessed for clinical effect. However, large-scale production of chemokines and cytokines is technically challenging,[37] and large quantities may be necessary to mediate *in vivo* effects. Here we harnessed the unique ability of the synDNA platform to parenterally co-deliver antigen and chemokine *in vivo*. Our results indicate that exposure of immune cells to antigen and mucosal chemokine alters the trafficking patterns of these cells and supports enhanced mucosal immunity *in vivo*.

SARS-CoV-2 infection occurs primarily at mucosal surfaces of the nose and throat. A major consequence of this infection is replication in the upper and lower lungs. Gut infection is also observed, with pathological sequelae.[38] Thus, generation of robust cellular and humoral responses at mucosal surfaces with parenteral vaccination could be an important area for development for SARS-CoV2 vaccines. Earlier reports have examined vaccine co-immunization with mucosal chemokine adjuvants. These studies examined the potential to affect peripheral or mucosal immune responses against HIV, and in non-human primates (NHP), enhanced viral control was observed after challenge in a subset of animals.[22] Studies in respiratory disease models were not performed, and statistical differences in mucosal IgA were not observed. Here we defined the effect of mucosal chemokine co-administration on peripheral and mucosal cellular and humoral responses and determined whether pCTACK co-immunization affected heterologous challenge with SARS-CoV-2 Delta variant virus.

Mice co-immunized with pCTACK exhibited dramatically increased T cell responses to wild-type SARS-CoV-2 spike peptides, as measured by IFNγ ELISpot assay, in their spleens and lungs compared with pS-only immunized animals. Recent studies have suggested that mucosa-homing $\alpha4\beta7^+$ T cells are decreased in individuals with COVID-19 independent of gastrointestinal symptoms, indicating a SARS-CoV-2-associated alteration of mucosal immune homeostasis. We observed increased mucosal frequencies of $\alpha4\beta7^+$ $CD8^+$ T cells in the lungs of pCTACK-co-immunized animals that secreted spike-specific IFNγ. Serum antibody responses were comparable between pS-only- and pCTACK-co-immunized animals, with both groups equally capable of binding wild-type SARS-CoV-2 RBD, producing similar IgG subtypes, and neutralizing wild-type spike-pseudotyped viruses *in vitro*. When we evaluated mucosal humoral responses, pS-only- and pCTACK-co-immunized animals had significantly more RBD-binding IgG in their cecal extracts than pVax-immunized animals. pCTACK-co-immunized animals had significantly more RBD-specific IgA in their cecal extracts than pS-only-immunized animals. We observed a positive correlation between serum IgG and cecal extract IgG, but we could not detect a correlation between serum IgA and cecal extract IgA, suggesting CTACK-induced mobilization of the mucosal immune system. When cecal extracts were used in the pseudovirus neutralization assay, pCTACK-co-immunized animal cecal extract exhibited a log higher neutralizing potency *in vitro* than cecal extracts from pS-only-immunized animals. Because both groups had similar IgG levels, these data illustrate that pCTACK-induced cecal extract pseudoviral neutralization is due to specifically increased antigen-specific mucosal IgA (Figure 2I).

We hypothesized that increased mucosal cellular and humoral responses might have significant effects on SARS-CoV-2 challenge outcomes in hACE2tg mice. Animals were immunized twice with pVax or pS or co-immunized with pCTACK, rested for 3 months, and then challenged with heterologous SARS-CoV-2 Delta variant virus. Similar to the outcomes observed in affected individuals, immunization with the wild-type spike plasmid afforded partial protection from Delta challenge. pS-only-immunized animals had significant weight loss, but most (60%) of these animals survived Delta challenge. When animals were co-immunized with pS and pCTACK, however, we observed no weight loss with no mortality so that 100% of pCTACK-co-immunized animals survived this heterologous challenge. As part of the challenge protocol, representative

Figure 3. pCTACK protects against morbidity and mortality in heterologous SARS-CoV-2 challenge

(A) Mice were immunized twice as in Figure 1 and rested for 3 months prior to challenge with 1×10^5 TCID50 SARS-CoV-2 (B.1.617.2; hCoV-19/Canada/ON-NML-63169/2021) and weight loss and survival were monitored longitudinally.

(B and C) SARS-CoV-2 wild-type (B) and Delta (B.1.617) (C) pseudovirus neutralization ID50 titers at day 72 post-2nd immunization. Four animals per group were euthanized at day 4 post-challenge to quantify viral loads.

(D and E) Replication-competent virus (D) and viral RNA (E) in the lungs 4 days post-infection.

(F–H) Weight loss as percent of initial weight for pVax (F), pS (G), and +pCTACK (H) co-immunized mice.

(I and J) Summary weight loss (I) and probability of survival (J) post challenge.

(K) Pathological scoring of lung sections from four mice.

(L) H&E and SARS-CoV-2 nucleocapsid staining of lung sections.

Each point represents the average of duplicate assays for an individual animals, horizontal lines represent the mean, and error bars represent the SEM (B–E). Lines represent individual animal (F–H) or averaged group weights (I). For (K), symbols represent individual animals, horizontal lines represent the mean, and error bars represent SD. *$p < 0.05$, **$p < 0.01$, ***$p < 0.001$, ****$p < 0.0001$ by Kruskall-Wallis ANOVA (B–E, K), Dunnett's multiple comparison test (I), or Mantel-Cox Log rank analysis (J). Data are representative of one experiment with n = 10 per group pre challenge, n = 4 per group at day 4 post-challenge, and n = 6 per group for weight loss and survival curves. Scale bars are 500 μm in low magnification and 200 μm in high magnification.

animals from each group were euthanized to quantify viral burden via TCID50 and qPCR on day 4 after challenge. We observed no significant differences in viral loads in the lungs by TCID50, with an important trend toward decreased viral RNA by qPCR at the time of euthanasia in the pCTACK-immunized group. Animals in this model display significant neuropathology, which is the primary cause of mortality. We did not observe any neuropathological symptoms among pCTACK-co-immunized animals; however, we were unable to address neuronal viral loads in the current study. When the lungs of mice were subjected to immunohistochemical analysis at the peak of infection, we observed interstitial pneumonia in control-immunized mice and pS-only immunized mice, but very minimal pneumonia was observed among pCTACK-co-immunized animals. These data strongly support robust mucosal immune control in the presence of pCTACK. pCTACK may mediate its protective effects by ameliorating infection-induced lung inflammation, protecting against disease. Our observations of increased T cell responses in the lungs of pCTACK-co-immunized animals support this hypothesis. However, we also observed a significant increase in mucosal IgA after pCTACK co-immunization, which suggests that pCTACK co-immunization may mediate disease control via enhancement of humoral and cell-mediated immunity at mucosal surfaces. These data suggest that directing vaccine-induced responses specifically to the mucosal compartment could have a significant effect on SARS-CoV2 infection outcomes. Further study of CTACK (CCL27) and possibly other chemokine adjuvants as adjuvants for SARS-CoV-2 vaccines is likely of importance.

Limitations of the study

A limitation of this study is that the overall mechanism of CTACK-mediated protection in heterologous virus challenge remains unclear. We observed that co-delivery of CTACK (CCL27) enhanced the frequency of IFNγ-secreting $\alpha4\beta7^+$ $CD8^+$ T cells in the lungs of co-immunized animals and increased antibody quantity and quality in the respiratory and gastrointestinal mucosae. This enhancement led to 100% protection from heterologous challenge with SARS-CoV-2 Delta variant virus, suggesting that mucosal chemokine adjuvants may enhance the breadth of anti-spike responses, but these studies did not define an underlying mechanism for this enhancement. Another limitation is the small number of animals euthanized 4 days after challenge to quantify viral loads. We observed a trend toward decreased lung viral loads in pCTACK co-immunized animals that was not statistically significant but supported by decreased lung pathology and viral antigen in the lungs (Figure 3). It is possible that CTACK co-immunization only enhanced the magnitude of anti-spike responses in the respiratory mucosa and that this enhancement limited viral dissemination and disease. However, we were unable to quantify viral load outside of the respiratory mucosa in these studies, which warrants further investigation. Finally, heterologous challenge with the Delta VOC was performed because this was the predominant circulating strain at the time of this study. Delta variant challenge models support robust, observable morbidity and mortality in hACE2tg mice. Studies to address the effect of mucosal chemokine adjuvants on protection against the current predominant strain, Omicron, as well as Omicron subvariants are ongoing. Models for Omicron and Omicron subvariant challenge are very recent and actively being validated for challenge. It will be important to study chemokine adjuvant effects in these new models as they are developed. Immunogenicity studies with early Omicron variant immunogens are in progress.

STAR★METHODS

Detailed methods are provided in the online version of this paper and include the following:

- KEY RESOURCES TABLE
- RESOURCE AVAILABILITY
  - Lead contact
  - Materials availability
  - Data and code availability
- EXPERIMENTAL MODELS AND SUBJECT DETAILS
  - Animals and immunization
  - Pseudovirus neutralization assay
  - SARS-CoV-2 challenge
- METHOD DETAILS
  - ELISpot assay
  - Intracellular cytokine staining and flow cytometry
  - ELISA
- QUANTIFICATION AND STATISTICAL ANALYSIS
  - Statistical analysis

ACKNOWLEDGMENTS

We thank the Animal Facility staff at The Wistar Institute and the Public Health Agency of Canada for providing care to the animals used in these studies. We also thank the flow cytometry core facility at The Wistar Institute. This work was supported by NIH NCI award T32 CA09171 (to E.N.G.) and NIH NIAID award T32-AI-055400 (to E.M.P.) and The Wistar Institute Coronavirus Discovery Fund, with additional support from CEPI/Inovio Pharmaceuticals. The graphical abstract was created in BioRender.

AUTHOR CONTRIBUTIONS

E.N.G., N.J.T., B.W., E.M.P., and D.B.W. designed experiments. E.N.G., E.M.P., and N.J.T. performed animal immunizations. E.N.G. and N.J.T. performed assays. B.W. and D.K. performed containment challenge and viral reproduction assays. C.E.-H. and E.M. performed histological analyses. The manuscript was written by E.N.G., N.J.T., C.E.-H., and B.W., with intellectual oversight from T.R.F.S., K.E.B., L.H., D.K., A.P., D.W.K., and D.B.W. The manuscript was submitted on behalf of all authors by E.N.G. and D.B.W.

DECLARATIONS OF INTERESTS

D.B.W. has received grant funding, participates in industry collaborations, has received speaking honoraria, and has received fees for consulting, including serving on scientific review committees and board series. Remuneration received by D.B.W. includes direct payments and stock or stock options. D.B.W. discloses the following paid associations with commercial partners: GeneOne (consultant), Geneos (advisory board), AstraZeneca (advisory board, speaker), Inovio (BOD, SRA, stock), Sanofi (advisory board), and BBI (advisory board).

Received: January 14, 2022
Revised: May 16, 2022
Accepted: June 23, 2022
Published: June 28, 2022

REFERENCES

1. Jo, D.-H., Minn, D., Lim, J., Lee, K.-D., Kang, Y.-M., Choe, K.-W., and Kim, K.N. (2021). Rapidly declining SARS-CoV-2 antibody titers within 4 months after BNT162b2 vaccination. Vaccines *9*, 1145. https://doi.org/10.3390/vaccines9101145.
2. Widge, A.T., Rouphael, N.G., Jackson, L.A., Anderson, E.J., Roberts, P.C., Makhene, M., Chappell, J.D., Denison, M.R., Stevens, L.J., Pruijssers, A.J., et al. (2021). Durability of responses after SARS-CoV-2 mRNA-1273 vaccination. N. Engl. J. Med. *384*, 80–82. https://doi.org/10.1056/nejmc2032195.
3. Naaber, P., Tserel, L., Kangro, K., Sepp, E., Jürjenson, V., Adamson, A., Haljasmägi, L., Rumm, P., Maruste, R., Kärner, J., et al. (2021). Declined antibody responses to COVID-19 mRNA vaccine within first three months.
4. Marot, S., Malet, I., Leducq, V., Zafilaza, K., Sterlin, D., Planas, D., Gothland, A., Jary, A., Dorgham, K., Bruel, T., et al. (2021). Rapid decline of neutralizing antibodies against SARS-CoV-2 among infected healthcare workers. Nat. Commun. *12*, 844. https://doi.org/10.1038/s41467-021-21111-9.
5. Bates, T.A., Leier, H.C., Lyski, Z.L., Goodman, J.R., Curlin, M.E., Messer, W.B., and Tafesse, F.G. (2021). Age-dependent neutralization of SARS-CoV-2 and P. 1 variant by vaccine immune serum samples. JAMA *326*, 868. https://doi.org/10.1001/jama.2021.11656.
6. Richards, N.E., Keshavarz, B., Workman, L.J., Nelson, M.R., Platts-Mills, T.A.E., and Wilson, J.M. (2021). Comparison of SARS-CoV-2 antibody response by age among recipients of the BNT162b2 vs the mRNA-1273 vaccine. JAMA Netw. Open *4*, e2124331. https://doi.org/10.1001/jamanetworkopen.2021.24331.
7. Baden, L.R., El Sahly, H.M., Essink, B., Kotloff, K., Frey, S., Novak, R., Diemert, D., Spector, S.A., Rouphael, N., Creech, C.B., et al. (2021). Efficacy and safety of the mRNA-1273 SARS-CoV-2 vaccine. N. Engl. J. Med. *384*, 403–416. https://doi.org/10.1056/nejmoa2035389.
8. Björk, J., Inghammar, M., Moghaddassi, M., Rasmussen, M., Malmqvist, U., and Kahn, F.J.I.D. (2021). High level of protection against COVID-19 after two doses of BNT162b2 vaccine in the working age population–first results from a cohort study in Southern Sweden. Infect. Dis. (Lond.), 1–6.
9. de Gier, B., Andeweg, S., Joosten, R., Ter Schegget, R., Smorenburg, N., van de Kassteele, J., RIVM COVID-19 surveillance and epidemiology team 1; van den Hof, S., de Melker, H.E., and Knol, M.J.; Members of the RIVM COVID-19 surveillance and epidemiology team (2021). Vaccine effectiveness against SARS-CoV-2 transmission and infections among household and other close contacts of confirmed cases, The Netherlands, February to May 2021. Euro Surveill. *26*, 2100640. https://doi.org/10.2807/1560-7917.es.2021.26.31.2100640.
10. de Gier, B., Andeweg, S., Backer, J.A., RIVM COVID-19 surveillance and epidemiology team; van den Hof, S., de Melker, H.E., and Knol, M.J.; RIVM COVID-19 surveillance and epidemiology team in addition to the named authors (2021). Vaccine effectiveness against SARS-CoV-2 transmission to household contacts during dominance of Delta variant (B.1.617.2), The Netherlands, August to September 2021. Euro Surveill. *26*, 2100977. https://doi.org/10.2807/1560-7917.es.2021.26.44.2100977.
11. Shin, H., and Iwasaki, A. (2013). Tissue-resident memory T cells. Immunol. Rev. *255*, 165–181. https://doi.org/10.1111/imr.12087.
12. Gary, E.N., and Kutzler, M.A. (2018). Defensive driving: directing HIV-1 vaccine-induced humoral immunity to the mucosa with chemokine adjuvants. J. Immunol. Res. *2018*, 1–14. https://doi.org/10.1155/2018/3734207.
13. Bernstein, D.I., Cardin, R.D., Bravo, F.J., Awasthi, S., Lu, P., Pullum, D.A., Dixon, D.A., Iwasaki, A., and Friedman, H.M. (2019). Successful application of prime and pull strategy for a therapeutic HSV vaccine. NPJ Vaccines *4*, 33. https://doi.org/10.1038/s41541-019-0129-1.
14. Shin, H., and Iwasaki, A. (2012). A vaccine strategy that protects against genital herpes by establishing local memory T cells. Nature *491*, 463–467. https://doi.org/10.1038/nature11522.
15. Kunkel, E.J., Kim, C.H., Lazarus, N.H., Vierra, M.A., Soler, D., Bowman, E.P., and Butcher, E.C. (2003). CCR10 expression is a common feature of circulating and mucosal epithelial tissue IgA Ab-secreting cells. J. Clin. Invest. *111*, 1001–1010. https://doi.org/10.1172/jci17244.
16. Xiong, N., Fu, Y., Hu, S., Xia, M., and Yang, J. (2012). CCR10 and its ligands in regulation of epithelial immunity and diseases. Protein Cell *3*, 571–580. https://doi.org/10.1007/s13238-012-2927-3.
17. Homey, B., Alenius, H., Müller, A., Soto, H., Bowman, E.P., Yuan, W., McEvoy, L., Lauerma, A.I., Assmann, T., Bünemann, E., et al. (2002). CCL27–CCR10 interactions regulate T cell–mediated skin inflammation. Nat. Med. *8*, 157–165. https://doi.org/10.1038/nm0202-157.
18. Homey, B., Wang, W., Soto, H., Buchanan, M.E., Wiesenborn, A., Catron, D., Müller, A., McClanahan, T.K., Dieu-Nosjean, M.C., Orozco, R., et al. (2000). Cutting edge: the orphan chemokine receptor G protein-coupled receptor-2 (GPR-2, CCR10) binds the skin-associated chemokine CCL27 (CTACK/ALP/ILC). J. Immunol. *164*, 3465–3470. https://doi.org/10.4049/jimmunol.164.7.3465.
19. Qiu, L., Huang, D., Chen, C., Wang, R., Shen, L., Shen, Y., Hunt, R., Estep, J., Haynes, B., Jacobs, Jr., W., et al. (2008). Severe tuberculosis induces unbalanced up-regulation of gene networks and overexpression of*IL-22, MIP-1*α*, CCL27, IP-10, CCR4, CCR5, CXCR3, PD1, PDL2, IL-3, IFN-*β*, TIM1,* and*TLR2*but low antigen-specific cellular responses. J. Infect. Dis. *198*, 1514–1519. https://doi.org/10.1086/592448.
20. Morteau, O., Gerard, C., Lu, B., Ghiran, S., Rits, M., Fujiwara, Y., Law, Y., Distelhorst, K., Nielsen, E.M., Hill, E.D., et al. (2008). An indispensable role for the chemokine receptor CCR10 in IgA antibody-secreting cell accumulation. J. Immunol. *181*, 6309–6315. https://doi.org/10.4049/jimmunol.181.9.6309.
21. Hu, S., Yang, K., Yang, J., Li, M., and Xiong, N. (2011). Critical roles of chemokine receptor CCR10 in regulating memory IgA responses in intestines. Proc. Natl. Acad. Sci. USA *108*, E1035–E1044. https://doi.org/10.1073/pnas.1100156108.
22. Kutzler, M.A., Wise, M.C., Hutnick, N.A., Moldoveanu, Z., Hunter, M., Reuter, M.A., Yuan, S., Yan, J., Ginsberg, A.A., Sylvester, A., et al. (2016). Chemokine-adjuvanted electroporated DNA vaccine induces substantial protection from simian immunodeficiency virus vaginal challenge. Mucosal Immunol. *9*, 13–23. https://doi.org/10.1038/mi.2015.31.
23. Gary, E., Kathuria, N., Makurumidze, G., Curatola, A., Ramamurthi, A., Bernui, M., Myles, D., Yan, J., Pankhong, P., Muthumani, K., et al. (2020). CCR10 expression is required for the adjuvant activity of the mucosal chemokine CCL28 when delivered in the context of an HIV-1 Env DNA vaccine. Vaccine *38*, 2626–2635. https://doi.org/10.1016/j.vaccine.2020.01.023.
24. Kraynyak, K.A., Kutzler, M.A., Cisper, N.J., Khan, A.S., Draghia-Akli, R., Sardesai, N.Y., Lewis, M.G., Yan, J., and Weiner, D.B. (2010). Systemic immunization with CCL27/CTACK modulates immune responses at mucosal sites in mice and macaques. Vaccine *28*, 1942–1951. https://doi.org/10.1016/j.vaccine.2009.10.095.
25. Gary, E.N., Warner, B.M., Parzych, E.M., Griffin, B.D., Zhu, X., Tailor, N., Tursi, N.J., Chan, M., Purwar, M., Vendramelli, R., et al. (2021). A novel mouse AAV6 hACE2 transduction model of wild-type SARS-CoV-2 infection studied using synDNA immunogens. iScience *24*, 102699. https://doi.org/10.1016/j.isci.2021.102699.
26. Kunkel, E.J., Campbell, J.J., Haraldsen, G., Pan, J., Boisvert, J., Roberts, A.I., Ebert, E.C., Vierra, M.A., Goodman, S.B., Genovese, M.C., et al. (2000). Lymphocyte CC chemokine receptor 9 and epithelial thymus-expressed chemokine (TECK) expression distinguish the small intestinal immune compartment: epithelial expression of tissue-specific chemokines as an organizing principle in regional immunity. J. Exp. Med. *192*, 761–768. https://doi.org/10.1084/jem.192.5.761.
27. Iwata, M., Hirakiyama, A., Eshima, Y., Kagechika, H., Kato, C., and Song, S.Y. (2004). Retinoic acid imprints gut-homing specificity on T cells. Immunity *21*, 527–538. https://doi.org/10.1016/j.immuni.2004.08.011.

28. Houshmand, P., and Zlotnik, A. (2003). Therapeutic applications in the chemokine superfamily. Curr. Opin. Chem. Biol. *7*, 457–460. https://doi.org/10.1016/s1367-5931(03)00086-3.

29. Kathuria, N., Kraynyak, K.A., Carnathan, D., Betts, M., Weiner, D.B., and Kutzler, M.A. (2012). Generation of antigen-specific immunity following systemic immunization with DNA vaccine encoding CCL25 chemokine immunoadjuvant. Hum. Vaccines Immunother. *8*, 1607–1619. https://doi.org/10.4161/hv.22574.

30. Sin, J.-I., Kim, J.J., Pachuk, C., Satishchandran, C., and Weiner, D.B. (2000). DNA vaccines encoding interleukin-8 and RANTES enhance antigen-specific Th1-type CD4+ T-cell-mediated protective immunity against herpes simplex virus type 2 in vivo. J. Virol. *74*, 11173–11180. https://doi.org/10.1128/jvi.74.23.11173-11180.2000.

31. Kutzler, M.A., Kraynyak, K.A., Nagle, S.J., Parkinson, R.M., Zharikova, D., Chattergoon, M., Maguire, H., Muthumani, K., Ugen, K., and Weiner, D.B. (2010). Plasmids encoding the mucosal chemokines CCL27 and CCL28 are effective adjuvants in eliciting antigen-specific immunity in vivo. Gene Ther. *17*, 72–82. https://doi.org/10.1038/gt.2009.112.

32. Aldon, Y., Kratochvil, S., Shattock, R.J., and McKay, P.F. (2020). Chemokine-adjuvanted plasmid DNA induces homing of antigen-specific and non–antigen-specific B and T cells to the intestinal and genital mucosae. J. Immunol. *204*, 903–913. https://doi.org/10.4049/jimmunol.1901184.

33. Khan, A.A., Srivastava, R., Vahed, H., Roy, S., Walia, S.S., Kim, G.J., Fouladi, M.A., Yamada, T., Ly, V.T., Lam, C., et al. (2018). Human asymptomatic epitope peptide/CXCL10-based prime/pull vaccine induces herpes simplex virus-specific gamma interferon-positive CD107+ CD8+ T cells that infiltrate the corneas and trigeminal ganglia of humanized HLA transgenic rabbits and protect against ocular herpes challenge. J. Virol. *92*, e00535-18. https://doi.org/10.1128/jvi.00535-18.

34. De Rosa, S.C., Edupuganti, S., Huang, Y., Han, X., Elizaga, M., Swann, E., Polakowski, L., Kalams, S.A., Keefer, M.C., Maenza, J., et al.; HIV Vaccine Trials Network HVTN 098 Study Team (2020). Robust antibody and cellular responses induced by DNA-only vaccination for HIV. JCI Insight *5*, 137079. https://doi.org/10.1172/jci.insight.137079.

35. Vonderheide, R.H., Kraynyak, K.A., Shields, A.F., McRee, A.J., Johnson, J.M., Sun, W., Chintakuntlawar, A.V., Pawlicki, J., Sylvester, A.J., McMullan, T., et al. (2021). Phase 1 study of safety, tolerability and immunogenicity of the human telomerase (hTERT)-encoded DNA plasmids INO-1400 and INO-1401 with or without IL-12 DNA plasmid INO-9012 in adult patients with solid tumors. J. Immunother. Cancer *9*, e003019. https://doi.org/10.1136/jitc-2021-003019.

36. Gray, J.E., Chiappori, A., Williams, C.C., Tanvetyanon, T., Haura, E.B., Creelan, B.C., Kim, J., Boyle, T.A., Pinder-Schenck, M., Khalil, F., et al. (2018). A phase I/randomized phase II study of GM. CD40L vaccine in combination with CCL21 in patients with advanced lung adenocarcinoma. Cancer Immunol. Immunother. *67*, 1853–1862. https://doi.org/10.1007/s00262-018-2236-7.

37. Veldkamp, C.T., Koplinski, C.A., Jensen, D.R., Peterson, F.C., Smits, K.M., Smith, B.L., Johnson, S.K., Lettieri, C., Buchholz, W.G., Solheim, J.C., and Volkman, B.F. (2016). Production of recombinant chemokines and validation of refolding. Methods Enzymol. *570*, 539–565. https://doi.org/10.1016/bs.mie.2015.09.031.

38. Lamers, M.M., Beumer, J., van der Vaart, J., Knoops, K., Puschhof, J., Breugem, T.I., Ravelli, R.B.G., Paul van Schayck, J., Mykytyn, A.Z., Duimel, H.Q., et al. (2020). SARS-CoV-2 productively infects human gut enterocytes. Science *369*, 50–54. https://doi.org/10.1126/science.abc1669.

STAR★METHODS

KEY RESOURCES TABLE

REAGENT or RESOURCE	SOURCE	IDENTIFIER
Antibodies		
anti-mouse CD8	Biolegend	Catalog number: 100742 RRID: AB_2563056
anti-mouse CD4	Biolegend	Catalog number: 100447 RRID: AB_2564586
anti-mouse CD3e	Biolegend	Catalog number: 100216 RRID: AB_493697
anti-mouse CD107a	Biolegend	Catalog number: 121606 RRID: AB_572007
anti-mouse IFNγ	Biolegend	Catalog number: 505810 RRID: AB_315404
Anti-mouse α4β7	Biolegend	Catalog number: 120606 RRID: AB_493267
anti-mouse IgG(h + l)-HRP	Bethyl	A90-216P
Bacterial and virus strains		
SARS-CoV-2; hCoV-19/USA/PHC658/2021	BEI resources	BEI cat# NR-55611
Chemicals, peptides, and recombinant proteins		
SARS-COV-2 spike peptides	Genscript	Custom peptide library created to match DNA plasmid antigens
Critical commercial assays		
Mouse IFNy ELISpot kit	Mabtech	3321-4APT-10
Experimental models: Cell lines		
CHO-ACE2 cell line	Creative Biolabs	VCeL-Wyb019
Recombinant DNA		
SARS-CoV-2 spike DNA plasmid	Genscript	N/A
Mouse CTACK (CCL27) DNA plasmid	Genscript	N/A
Software and algorithms		
Prism v. 9	Graphpad	V9.1.1(225)
Flowjo v.10	Treestar	v10.7.2

RESOURCE AVAILABILITY

Lead contact

Further information and requests for resources and reagents should be directed to lead contact, Dr. David B. Weiner at the Wistar Institute (dweiner@wistar.org).

Materials availability

This study generated unique DNA plasmid immunogens and matched peptides as well as ACE2-expressing modified AAV6 vectors and SARS-CoV-2 pseudotyped viruses, all of which are proprietary. Reasonable requests for materials will be made available by request to David B. Weiner (dweiner@wistar.org).

Data and code availability

The published article includes all datasets generated or analyzed during this study.
All data in this paper will be shared by the lead contact upon request
This paper does not report original code
And additional information required to reanalyze the data reported in the paper is available upon request.

EXPERIMENTAL MODELS AND SUBJECT DETAILS

Animals and immunization

BALB/c and human ACE2 transgenic (K18) were purchased from The Jackson Laboratory and were housed in the Wistar Institute Animal Facility. 40ug total of DNA (40ug empty plasmid vector (pVax), 10μg of DNA plasmid encoding SARS-CoV-2 Spike glycoprotein (pS) with 30ug of pVax (30ug), or 10ug of pS and 30ug of mouse CTACK DNA (+pCTACK) in 30μL water was injected in the tibialis

anterior (TA) muscle, followed by delivery of two 0.1 Amp electric constant current square-wave pulses by the CELECTRA-3P electroporation device (Inovio Pharmaceuticals) to increase transfection efficiency. In some experiments control animals were immunized with 10ug of pVax and 30ug of pCTACK. The vaccine schedule is indicated in each figure. All procedures were done in accordance with the guidelines from the Wistar Institute Animal Care and Use Committee. Blood via cardiac puncture, spleens, and Bronchoalveolar lavage (BAL) fluid were collected at the time of euthanasia.

Pseudovirus neutralization assay

SARS-CoV-2 pseudovirus were produced using HEK293T cells transfected with 1:1 ratio of IgE-SARS-CoV-2 S plasmid (Genscript) and pNL4-3.Luc.R-E− plasmid (NIH AIDS reagent)using Gene jammer (Agilent) as transfection reagent. Forty-eight hours post transfection, transfection supernatant was collected, enriched with FBS to 12% final volume, and stored at −80°C. SARS-Cov-2 pseudovirus neutralization assay was set up using D10 media (DMEM supplemented with 10%FBS and 1X Penicillin-Streptomycin) in a 96 well format using huCHOAce2 cells (Creative Biolabs, Catalog No. VCeL-Wyb019). For neutralization assay, 10,000 CHO-ACE2 cells were plated in 96-well plates and rested overnight at 37°C and 5% CO2 for 24 h. Following day, sera, bronchoalveolar lavage (BAL), or cecal extracts from vaccinated and control groups were heat inactivated and serially diluted as desired. Sera were incubated with a fixed amount of SARS-Cov-2 pseudovirus for 90 min at RT following which the mix was added to huCHOAce2 cells and allowed to incubate in a standard incubator (37% humidity, 5% CO2) for 72h. Post 72h, cells were lysed using britelite plus luminescence reporter gene assay system (Perkin Elmer Catalog no. 6066769) and RLU were measured using the Biotek plate reader. Neutralization titers (ID50) were calculated using GraphPad Prism 8 and defined as the reciprocal serum dilution at which RLU were reduced by 50% compared to RLU in virus control wells after subtraction of background RLU in cell control wells.

SARS-CoV-2 challenge

For challenge with SARS-CoV-2, all mice were anesthetized with inhalation isoflurane. Virus (SARS-CoV-2; hCoV-19/USA/PHC658/2021) was diluted in plain media and animals were administered 10^5 $TCID_{50}$ intranasally in 50μL (25μL per nare). Animals were recovered and then weighed and monitored daily for any clinical signs of disease. On day 4 post-infection, animals were euthanized to examine viral replication in the respiratory tract. Euthanasia was performed by cervical dislocation following anesthesia with inhaled isoflurane.

METHOD DETAILS

ELISpot assay

Spleens from immunized mice were harvested and stored in RPMI 1640 media (Invitrogen) before being dissociated by a stomacher. Red blood cells were removed by ACK lysing buffer. The splenocytes were filtered and counted. 2×10^5 splenocytes were plated into each well on Mouse IFN-γ ELISpot^{PLUS} plates (Mabtech) and stimulated for 20 h with SARS-CoV-2 spike peptides (15-mer peptides overlapping by 9 amino acids). Cells were stimulated with 5 μ g/mL of each peptide in complete media (R10). The spots were developed based on manufacturer's instructions. R10 and cell stimulation cocktails (Invitrogen) were used for negative and positive controls, respectively. Spots were scanned and quantified by ImmunoSpot CTL reader. Spot-forming unit (SFU) per million cells was calculated by subtracting the negative control wells.

Intracellular cytokine staining and flow cytometry

Wells were seeded with 1,000,000 cells in 100 μL of R10. Cells were stimulated with peptides from SARS-CoV-2 at a final concentration of 5 μg/mL per peptide in the presence of Protein Transport Inhibitor (eBioscience, San Diego, CA, USA). R10 and Cell Stimulation Cocktail (eBioscience, San Diego, CA, USA) were used as negative and positive controls, respectively. Plates were incubated for 5 h at 37°C with 5% CO_2.Splenocytes were stimulated by peptides for 5 h with protein transport inhibitor (Invitrogen). After stimulation, cells were stained with LIVE/DEAD violet for viability. CD3e (17A2), CD4 (RM4-5), CD8b (YTS156.7.7), IFN-γ (XMG1.2), α4β7(DATK32), and IL-2 (JES56-5H4) fluorochrome conjugated antibodies (all from BioLegend) were used for surface and intracellular staining. The samples were run on an 18-color LSRII flow cytometer (BD Biosciences) and analyzed by FlowJo software. Gates were set using FMOs for each stain. Data were exported and analyzed in GraphPad Prism 8.1.1.

ELISA

For binding and quantification of serum and BAL antibodies, NUNC MaxiSorp 96-well plates (Thermo Scientific) were coated with 1 μg/mL RBD of SARS-CoV-2 spike protein (Genscript) in PBS overnight at 4°C. The following day, plates were washed with PBS-0.5% Tween 20 and blocked with PBS-10% fetal bovine serum. Next, the plates were again washed and subsequently incubated with diluted mouse sera for 2 h. Following primary serum incubation, plates were incubated with goat anti-mouse IgG-HRP (Bethyl) for 1 h at room temperature. TMB (Thermo) was used to develop the binding signal. Upon stopping with 1N sulfuric acid, plates were read with the BioTek Synergy 2 plate reader (BioTek) at 450nm. Data were subsequently exported to Microsoft Excel and analyzed in graphpad prism version 8.

QUANTIFICATION AND STATISTICAL ANALYSIS

Statistical analysis

All statistics were analyzed using GraphPad Prism 8. Error bars represent means ± SEM or the mean ± SD where denoted. Normality was determined using the Shapiro-Wilk normality test. Outliers were determined and removed using the ROUT algorithm. For data deemed normal, ordinary one-way analysis of variance (ANOVA) was performed to determine statistical significance between groups of three or more (Tukey's multiple comparison test). For data deemed non-normal, a non-parametric Kruskal-Wallis test was performed in order to determine statistical differences between groups of three or more. Statistical differences between groups of two were determined via unpaired t test for data deemed normal, or Mann-Whitney U test for data deemed non-normal. In all data *$p < 0.05$, **$p < 0.01$, ***$p < 0.001$, and ****$p < 0.0001$.